BURN-UP OF FUSION-PRODUCED TRITONS AND ^{3}He IONS IN PLT AND PDX

W.W. HEIDBRINK, R.E. CHRIEN, J.D. STRACHAN
Plasma Physics Laboratory,
Princeton University,
Princeton, New Jersey,
United States of America

ABSTRACT. The d(d,p)t and d(d,n)^{3}He fusion reactions produce 1 MeV tritons and 0.8 MeV ^{3}He ions which can subsequently undergo d(t, n) α and d(^{3}He, p) α fusion reactions. The magnitude of this triton and ^{3}He ion 'burn-up' was measured on the PLT and PDX tokamaks by detection of the 14 MeV neutron and 15 MeV proton emission. In discharges with $B_\phi > 2$ T, the measured ^{3}He and triton burn-up is consistent (within a factor of three) with predictions based on classical theories of ion confinement and slowing down. In discharges with weaker toroidal fields but constant plasma current, the burn-up of both ions fell by more than a factor of ten so that the observed burn-up was significantly less than expected classically.

1. INTRODUCTION

The properties of MeV ions in fusion devices are of interest since ignition requires that charged fusion reaction products be confined long enough for most of their energy to be transferred to the plasma. Previously, confinement of 1 MeV tritons in the PLT tokamak was reported [1] in the first investigation of fusion reaction product confinement in a tokamak. In this paper, those results are extended to include more accurate triton confinement diagnostics. In addition, the first measurements of the confinement of 0.8 MeV ^{3}He ions produced by the d(d,n) ^{3}He fusion reaction are reported.

During injection of beams of 40–50 keV deuterium neutrals into PLT or PDX discharges, 1.0 MeV tritons and 0.8 MeV ^{3}He ions are produced primarily by beam-target d(d,p)t and d(d,n) ^{3}He fusion reactions at rates of $10^{13} - 10^{14}$ s^{-1} [2]. The 1 MeV triton and 0.8 MeV ^{3}He production rates are nearly equal to the 2.5 MeV neutron rate (Fig.1) that is usually used to monitor the d-d fusion reactions. These 1 MeV tritons and 0.8 MeV ^{3}He ions can subsequently burn up through d(t, n) α and d(^{3}He,p) α fusion reactions as they slow down through the maximum of their respective cross-sections. The fraction of tritons that produce 14 MeV neutrons and the fraction of ^{3}He ions that produce 14.7 MeV protons are a sensitive function of the confinement of these ions since the probability of undergoing a fusion reaction is about 10^4 times as great for an ion that slows down classically in the plasma as for an ion that escapes the plasma and encounters sorbed deuterium in the vessel walls. Since the resonance of the fusion reaction cross-section for the triton is at lower energy than for the ^{3}He ion (Fig.1), the triton burn-up is more sensitive to non-prompt losses than the ^{3}He burn-up.

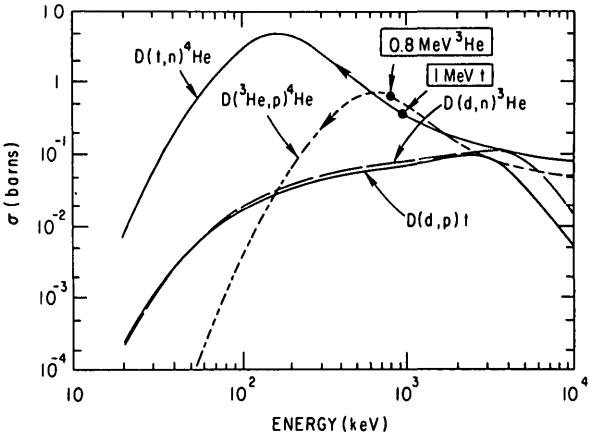

FIG.1. Fusion reaction cross-sections. The 1 MeV triton and 0.8 MeV ^{3}He ion slow down through the peak of the d(t, n) and d(^{3}He, p) cross-sections.

The fraction of tritons that burned up through the d(t, n) α fusion reaction when the toroidal field was 3.2 T was about 6 X10^{-4}, a value that is consistent with the predictions of classical orbit and slowing-down theory. The measured value of the triton burn-up was a factor of eight less than in previous

PLT measurements [1]; the difference is probably due primarily to the greater accuracy of the diagnostic techniques employed here. The ^{3}He burn-up measured at 2.2 T was about 3×10^{-4}, which is also consistent with classical theory. However, when the toroidal field was halved and the plasma current was held constant, the burn-up of both the triton and the ^{3}He ion dropped by over an order of magnitude. Classically, the burn-up is expected to fall only modestly when the toroidal field is reduced.

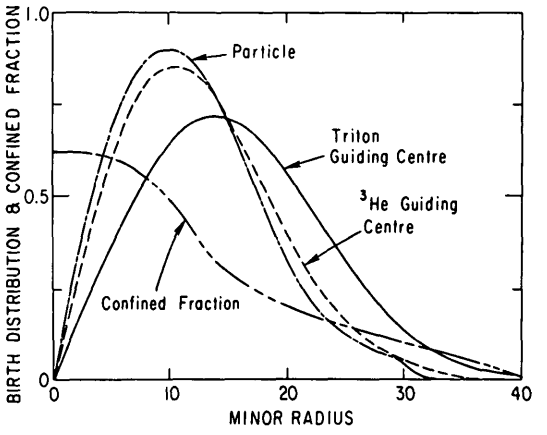

FIG.2. Effective guiding-centre birth distributions rS(r) for a broad PLT d-d reaction profile (200 kA, 2.2 T, parabolic density and temperature). The particle birth profile is determined by solution of the Fokker-Planck equation for beam ions [2, 3]. Also shown is the fraction of tritons confined in PLT (MIS code, 500 kA) as a function of minor radius.

2. THEORY

2.1. Classical burn-up

Most fusion-produced tritons and ^{3}He ions are born near the hot centre of the plasma (Fig.2) [2, 3]. Many of these energetic ions are born on orbits that strike the limiter and promptly escape from the plasma. (In contrast, in a reactor, the first orbit losses are expected to be small.) Classically, the fraction of fusion products that remains confined in the plasma is a function of the magnitude and distribution of the plasma current (Fig.3) as well as of the spatial birth distribution. Confined MeV ions slow down predominantly owing to collisions with electrons, losing energy in a time approximately proportional to $T_e^{3/2}/n_e$ [4]. While slowing down, about 5×10^{-3} tritons and 3×10^{-4} ^{3}He ions undergo d-t and d-^{3}He fusion reactions for PLT conditions. The classical burn-up probability scales approximately as $n_d T_e^{3/2}/n_e$, where n_d is the deuteron density.

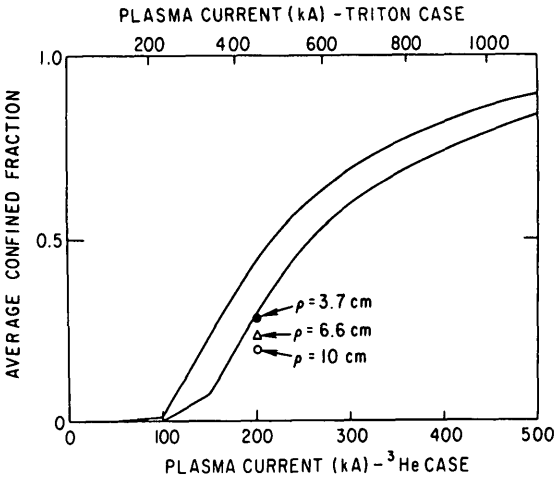

FIG.3. Fraction of 1.0 MeV tritons (upper scale) and of 0.82 MeV ^{3}He ions (lower scale) confined in PLT ($a/R_0 = 0.30$), as a function of plasma current. Current profiles of the form $j \propto [1-(r/a)^2]^i$ are assumed. The curves were calculated assuming zero gyroradius (MIS code) for peaked ($i = 6$) and broad ($i = 3$) current profiles (upper and lower curves, respectively). The points were calculated by the SGA code for an intermediate ($i = 4$) current profile. The birth distribution was of the form $rS(r) = r[1-(r/a)^2]^6$.

To evaluate the burn-up of classically behaved ions, one should solve the Fokker-Planck equation for the triton or ^{3}He distribution function, $f(\vec{r}, \vec{v}, t)$, subject to the 'boundary' conditions that these MeV ions are produced at the rate $R(\vec{r}, \vec{v}, t)$ and lost when they either thermalize or strike the walls. $f(\vec{r}, \vec{v}, t)$ is used together with the deuterium distribution function to calculate the d(t, n) α or d(^{3}He, p) α reaction rate. The principal difficulty in solving the full Fokker-Planck equation is that MeV ion orbits are large and complex so that the drag and diffusion coefficients in the equation must be determined numerically; in the two codes employed here, simplifying approximations are made in the calculations of these coefficients.

In the first of these codes, the actual fusion product orbits are approximated by their drift orbits in the calculation of prompt losses to the limiter [5]; any MeV ion that drifts outside the limiter radius is considered lost. The rate of energy loss is computed using the Coulomb drag experienced by the MeV ion at its birth position rather than the drag along its actual orbit. The approximations underestimate the prompt losses and the Coulomb drag, so that this 'modified in situ'

(MIS) code can considerably overestimate the burn-up [6]. This fast, simple code is used here to examine the parametric dependences of the burn-up.

For accurate, quantitative comparison with the experiment, a more time-consuming code is used. In this code, prompt losses are calculated using the full MeV ion orbit. The Coulomb drag is assumed to be the average drag felt by the MeV ion in its first full poloidal orbit including gyromotion. Since slowing down causes the orbits to contract into the centre of the plasma, this 'single gyro-orbit approximation' (SGA) code overestimates the Coulomb drag. A comparison of this first orbit approximation with more accurate Monte-Carlo calculations of energy loss for an analogous problem [6] indicates that, in the zero gyroradius limit, the SGA code only slightly underestimates the MeV ion burn-up.

Since less than 1% of the MeV ions are expected to pitch-angle-scatter into the loss cone [7], both codes neglect this effect. Estimates of the effect of energy diffusion, of Doppler broadening, of deuterium temperature and velocity, and of charge-exchange losses indicate that these processes are also of negligible importance.

The guiding-centre Monte-Carlo code [8] of Ref.[1] yields burn-up predictions intermediate between that of the MIS code and that of the SGA code in the zero gyroradius limit (Fig.4). The SGA code is the more accurate, however, since it employs the full ion gyro-orbit. The large gyroradius of the MeV ions (11 cm for the 1 MeV triton and 5 cm for the 0.8 MeV ^{3}He ion at 2.2 T) typically reduces the burn-up by 25% for the ^{3}He ion and by 100% for the triton at 2.2 T. Three separate finite gyroradius effects are responsible for this reduction. First, since particles are born initially with random gyrophase, their guiding centres are displaced by a gyroradius from their birth position. This implies that the guiding-centre birth distribution is broader by roughly a gyroradius than the particle birth distribution (Fig.2). Since guiding centres born farther from the centre of the discharge are more poorly confined than centrally born guiding centres, a broader birth distribution results in increased prompt losses of MeV ions. A second finite gyroradius effect is that the effective limiter radius is reduced for fusion products since ions that execute a drift orbit passing within a gyroradius of the limiter are lost. A third effect of finite gyroradius is increased net electron drag due to larger orbits that sample colder plasma regions.

^{3}He ions take 12 ms to slow down through the peak of the fusion reaction cross-section for T_e = 1 keV and

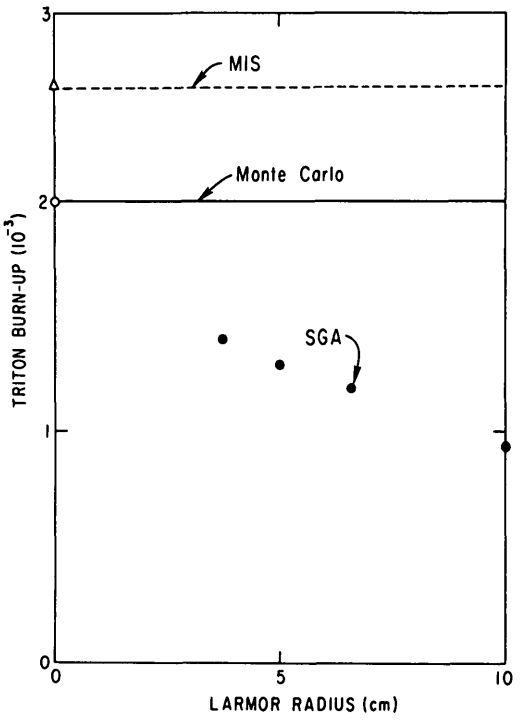

FIG.4. Comparison of the triton burn-up calculated by the MIS code, the guiding-centre Monte-Carlo code of Refs [1, 8] and the SGA code. The comparison is for a highly peaked PLT birth distribution (essentially all tritons born within 15 cm of the plasma centre) in a deuterium plasma with $T_e(r) = 2$ keV $[1-(r/a)^2]^4$. The current profiles used are not strictly identical ($I_\phi = 444$ kA, $j \propto [1-(r/a)^2]^4$ for the SGA code and $I_\phi = 400$ kA, $j \propto [1-(r/a)^2]^6$ for the Monte-Carlo code). The MIS code predicts the same burn-up for either of these distributions, however, so the difference is not significant.

$n_e = 3.5 \times 10^{13}$ cm^{-3}; the cross-section-weighted slowing-down time for tritons is 95 ms. In the discharges studied, the plasma current and d-d reaction rate were nominally constant during the 150–200 ms of neutral beam injection. The plasma density generally rose steadily, while the electron temperature rose in ~30–50 ms to a nominal steady state. After neutral beam injection, the electron temperature typically fell in about the energy confinement time to its Ohmic level; the plasma current also decreased after the beam pulse. Inclusion of the actual time evolution of the plasma parameters in the burn-up calculation typically reduces the predicted triton burn-up by 20% and the ^{3}He burn-up by less than 5% relative to a steady-state calculation.

Major uncertainties in the theoretical predictions are associated with uncertainties in the experimental input to the calculations. The calculated burn-up is

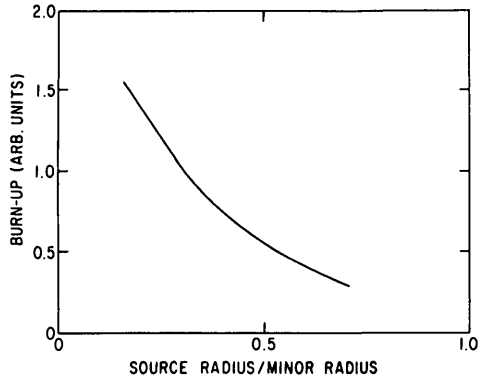

FIG.5. Sensitivity of the ^{3}He burn-up to the width of the birth distribution in a deuterium plasma with $I_\phi = 200$ kA, $j \propto [1-(r/a)^2]^4$, $B_\phi = 2.2$ T, $T_e \propto [1-(r/a)^2]^3$, as calculated by the SGA code. Half of the ^{3}He ions in a birth distribution of the form $rS(r) \propto r[1-(r/a)^2]^i$ are born inside the 'source radius' plotted on the abscissa. This radius is typically 0.2 – 0.3 for a neutral-beam-produced beam-target distribution.

quite sensitive to the MeV ion birth distribution (Fig.5), which was not measured in the experiments reported here. Variations in the spatial distribution of d-d reactions that result in a factor-of-two uncertainty in the theoretical burn-up predictions are consistent with the nearly classical neutron emission usually observed for $D^0 \rightarrow D^+$ discharges in PLT [2]. Uncertainties in the current distribution and in the ratio of deuteron density to electron density also result in considerable uncertainty in the theoretical predictions.

2.2. Anomalous burn-up

Anomalously small values of the burn-up can be observed if one or more of the following processes occur:

(a) Prompt losses exceed those calculated by orbit theory
(b) Non-prompt losses occur on a time-scale comparable to, or faster than, the time required for the MeV ions to slow down through the maximum of the fusion cross-section
(c) Slowing down proceeds at a faster rate than predicted by Coulomb scattering theory.

We have developed phenomenological models for anomalous burn-up. These models are:

(a) *Effective loss radius model.* In this model, anomalous prompt losses are related to a reduced 'effective limiter radius' by assuming that any ion whose guiding centre reaches a certain minor

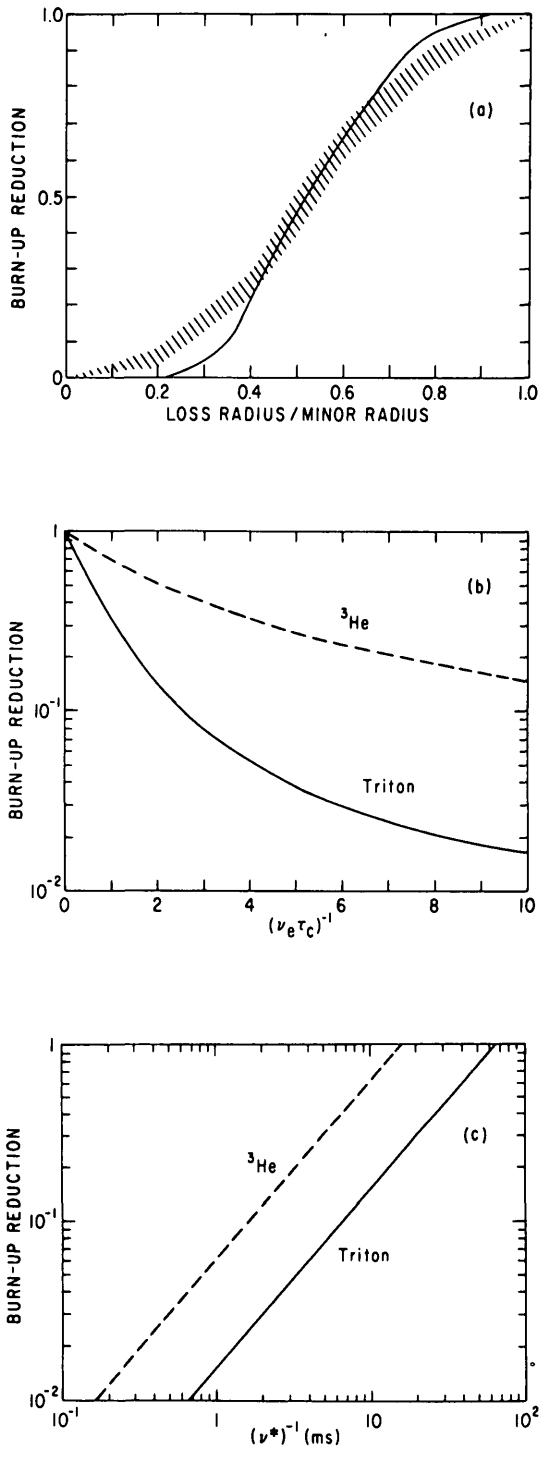

FIG.6. (a) Fraction of tritons or ^{3}He ions with drift orbits (MIS code) that do not extend beyond a_{eff} normalized to the fraction confined within $r = a$ for typical PLT current and birth distribution (hatched area). The curve is the burn-up reduction as a function of effective limiter radius calculated by a code that includes finite Larmor radius effects (SGA code) for the case of ^{3}He ions at $I_\phi = 200$ kA and $B_\phi = 1.7$ T. (b) Reduction in reaction probability as a function of the confinement time τ_c. (c) Reduction in burn-up at $T = 1$ keV, $n = 3 \times 10^{13}$ cm^{-3}, as a function of the energy loss time $(\nu^*)^{-1}$.

radius is lost (Fig.6(a)). The model simulates physical processes such as intrinsic orbit stochasticity due to magnetic field perturbations that cause 'confined' classical orbits to actually be loss orbits.

(b) *Confinement time model.* To mimic non-prompt losses, the density of MeV ions in a beam of particles created at t = 0 is assumed to decrease as $n(t) = n_0 e^{-t/\tau_c}$, where τ_c is the (constant) 'confinement time'. In Fig.6(b) the reduction in burn-up is plotted as a function of τ_c^{-1} normalized to ν_e, the electron drag rate evaluated at the fusion-product birth energy. This model simulates diffusive ion losses through a process such as $\vec{E} \times \vec{B}$ drifts due to plasma turbulence.

(c) *Enhanced drag model.* To mimic anomalous slowing down, the slowing down is assumed to be enhanced by a constant factor $\nu^* = k\nu_e$, $E = E_0 e^{-\nu^* t}$. The reduction in burn-up is then simply $B/B_0 = \nu_e/\nu^*$ (Fig.6(c)). This model simulates energy loss to plasma waves or stronger than classical electron-ion coupling.

3. DETECTION METHODS

3.1. 1 MeV tritons

In order to measure the d-t/d-d neutron emission ratio, it would be desirable to have a detector which is sensitive to 14 MeV neutrons (fluxes of $10^1 - 10^5$ cm^{-2}·s^{-1}) and insensitive to 10^4 times higher fluxes of 2.5 MeV neutrons, 10^3 times higher fluxes of epithermal neutrons and ~10^5 times higher fluxes of hard X-rays (0.1 – 20 MeV).

In the absence of such a detector, we have used threshold activation samples, which constitutes a simple and accurate selective neutron diagnostic method providing excellent discrimination against lower-energy neutrons and hard X-rays. The d-d neutron emission was measured with indium activation samples [9] to about 30% accuracy. The d-t neutrons were selectively detected with a sample (aluminium) for which the neutron activation threshold is greater than 2.5 MeV and for which the final (radioactive) product of the reaction cannot be produced by other neutron or hard X-ray reactions in the sample material. The disadvantages of these activation sample measurements are that they provide no time resolution and are rather insensitive. The absence of time resolution prevents us from assessing the influence of single shot variations in triton confinement and burn-up.

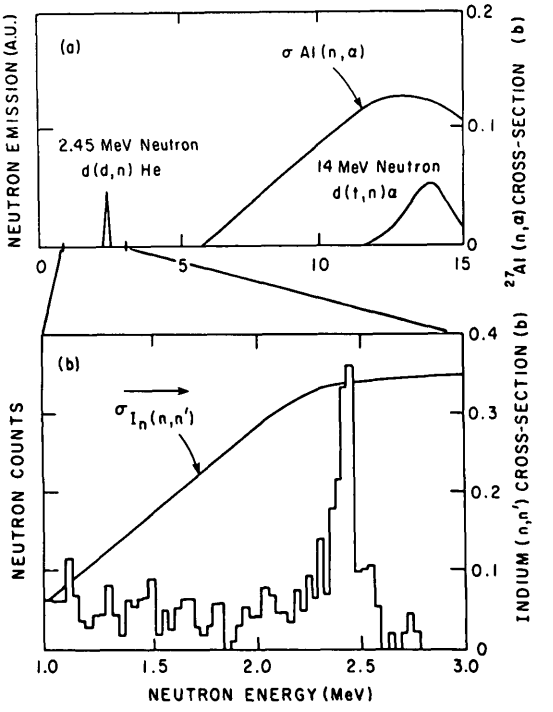

FIG.7. (a) Cross-section for the $^{27}Al(n,\alpha)$ reaction, together with the expected Doppler-broadened emission of 2.4 MeV and 14.0 MeV neutrons. (b) Cross-section for the $^{115}In(n,n')$ reaction and the PLT neutron spectrum to which the indium sample is exposed, as measured by a collimated ^3He ionization chamber [9]. Counts below the peak centred at 2.5 MeV are generated by scattered neutrons.

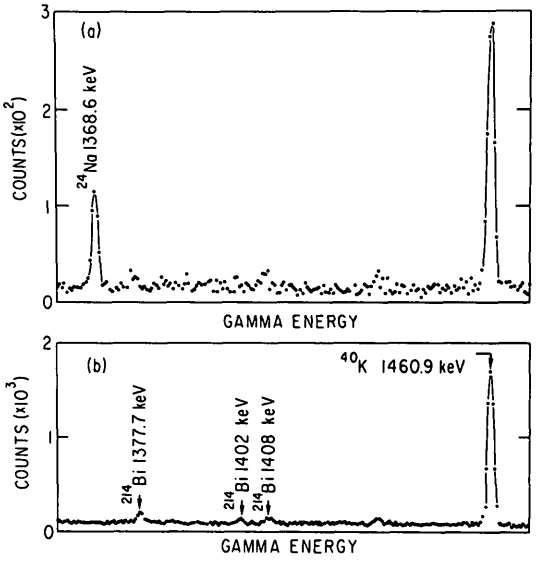

FIG.8. (a) Gamma spectrum for one aluminium activation sample exposed on PLT. The ^{24}Na peak is due to d-t neutrons. (b) Background spectrum.

The reaction $^{27}Al(n,\alpha)^{24}Na$ has a neutron threshold of 3.25 MeV and a cross-section of 1.2×10^{-25} cm^2 at 14 MeV (Fig.7). The ^{24}Na β^- decays to ^{23}Na with a half-life of 15.02 h by emitting two gammas (1.369 and 2.754 MeV). The lower-energy gammas were detected with a high-purity germanium gamma spectrometer (Gamma-X, EG&G Ortec) (Fig.8). A possible source of contamination for the aluminium sample would be sodium, due to $^{23}Na(n,\gamma)^{24}Na$ thermal or epithermal neutron activation. The aluminium samples were tested for ^{23}Na impurity by exposing them for one hour to a thermal neutron reactor beam with a flux of 8.4×10^{10} cm$^{-2} \cdot$s^{-1}. We found that the sodium impurity was less than 1.5×10^{-5}, which presents no interference with our d-t activation measurements.

For measurements of the d-t neutron emission, the aluminium samples were located at the vacuum vessel wall on the horizontal midplane and exposed to 10–100 tokamak discharges. Because of the low sensitivity of the activation method, these samples were useful only at the highest neutron emission levels during several megawatts of deuterium neutral beam injection heating.

The 2.5 MeV neutron emission level was monitored by placing an indium activation foil [9] at the same location as the aluminium sample. The two threshold reactions have about the same energy dependence with respect to the two neutron emissions so that the scattered neutrons of degraded energy are roughly of equal importance in each activation sample (Fig.7).

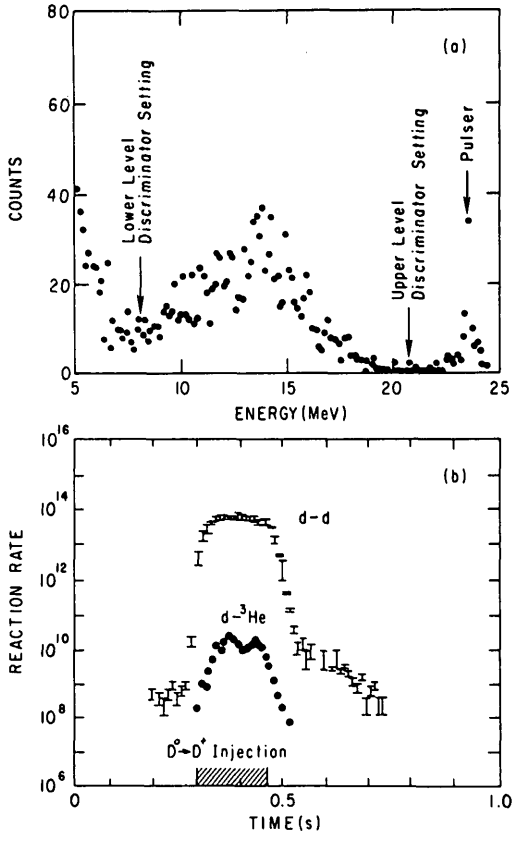

FIG.9. (a) Spectrum obtained with a silicon surface barrier detector showing the d-^{3}He proton peak. The 14.7 MeV protons lose ⩾ 2.2 MeV of energy in a 0.13 mm stainless steel foil; the Doppler-broadened peak is expected to extend from 11 to 15 MeV. The counts below 7 MeV and the broadening of the calibrated pulser signal are due to electronic and X-ray noise. The foil eliminates soft X-ray and plasma light noise. (b) Time evolution of the PDX d-d and d-^{3}He emissions.

3.2. 0.8 MeV ^{3}He ions

The ratio of d-^{3}He/d-d reactions was measured by determining the ratio of 14.7 MeV proton emission to 2.5 MeV neutron emission. Although the emission ratio is only $\sim 10^{-4}$ (Fig.9), detection of the 15 MeV proton is easier than detection of the 14 MeV neutron since charged-particle detectors exist that can discriminate well against neutron and X-ray radiations. Time-resolved measurements of the 15 MeV proton emission are made with a silicon surface barrier detector [10]. The principal uncertainty in the determination of the ^{3}He burn-up is in the absolute calibration of the d-^{3}He emission, which was calculated from the detector entrance aperture, and the probability that a 15 MeV proton will have an orbit that leaves the plasma and passes through the detector aperture. The spatial dependence of the reaction rate is not measured experimentally, although it is probably centrally peaked like the d-d reaction rate. A sensitivity analysis indicates that the uncertainty in the calculated detector efficiency is ±40%, owing to uncertainties in the birth profile.

We have confirmed the validity of this calculation with a ^{3}He gas puffing experiment on PLT similar to that of Ref.[11]. In this experiment, ^{3}He gas was puffed into a nominally deuterium plasma during injection of deuterium neutral beams. The ^{3}He density in the plasma was estimated from the rise in electron density associated with the gas puff (Fig.10). Under these conditions, both the ^{3}He(d,p)α reaction rate $R_{d\text{-}^3He}$ and the d(d,n)^{3}He rate $R_{d\text{-}d}$ are due primarily to beam-target reactions. Therefore, $R_{d\text{-}^3He}$ is given approximately by

$$R_{d\text{-}^3He} \cong \frac{n_{^3He}}{n_d} \frac{\langle \sigma_{dHe} v \rangle}{\langle \sigma_{dd} v \rangle} R_{d\text{-}d} \qquad (1)$$

The d(d,n)^{3}He reaction rate was measured using the 2.5 MeV neutron emission. The deuterium density was estimated from the electron density before the puff; it is, however, different from the electron density owing to hydrogen and higher-Z impurities in the plasma. Measurements of the molecular deuterium and hydrogen concentrations made a few seconds after the discharge found more hydrogen molecules than

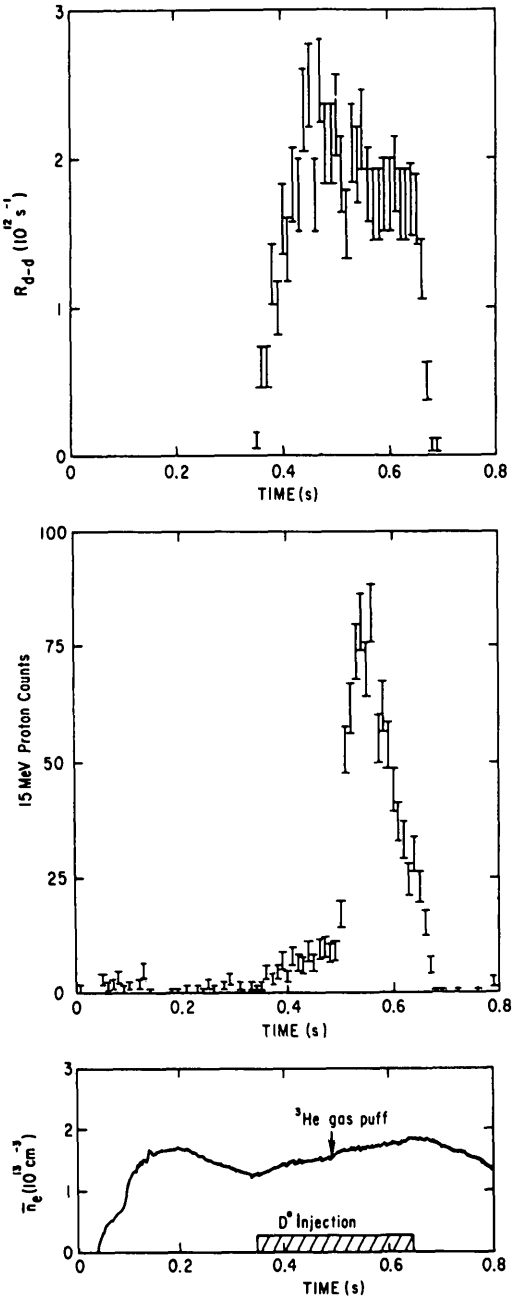

FIG.10. Time evolution of the d(d, n) ^{3}He and ^{3}He(d, p)α emissions and of the electron density during the ^{3}He gas puffing experiment.

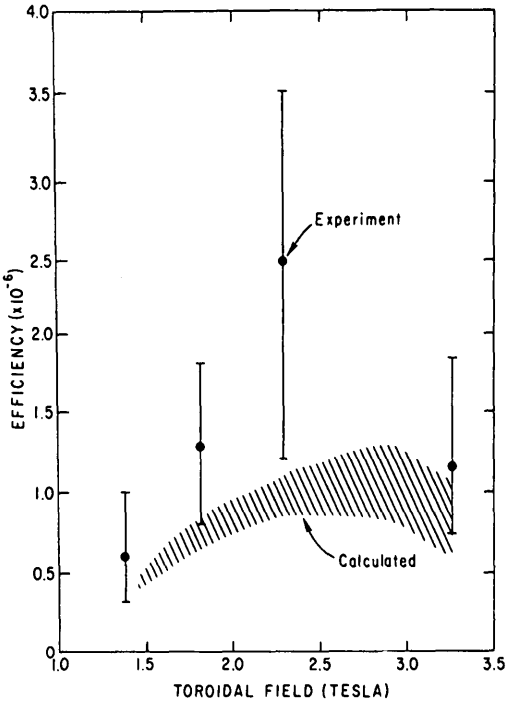

FIG.11. Comparison of the 15 MeV proton detection efficiency deduced from the ^{3}He gas puffing experiments with the calculations of detector efficiency.

deuterium molecules in the vessel chamber. We have assumed that $n_d = 0.5\ n_e$, and an uncertainty in the calibration of a factor of two is due to this assumption.

Within experimental error, the gas puffing experiment confirms the calculated detector efficiency (Fig.11). Using the efficiency calculation, the absolute error of the ^{3}He burn-up measurements is ± 70%. Also, we note that the detector efficiency is relatively insensitive to the toroidal magnetic field (Fig.11).

4. RESULTS

The data reported here were collected during deuterium neutral beam injection into both PLT and PDX for the triton burn-up and into PDX for the ^{3}He burn-up. PDX has an advantage over PLT in the study of ^{3}He ion burn-up since ^{3}He gas has never been introduced into the PDX vessel, whereas ^{3}He has often been used in PLT ICRF studies. Tritium gas has not been introduced into either the PLT or PDX vessels. In these studies, PDX and PLT were run with carbon limiters at 44 and 40 cm minor radius, respectively. The beam injection angle was near perpendicular on PDX with up to 4 MW of power, while tangentially

injected neutral beams were employed on PLT with up to 2 MW of power. Whenever possible, $D^0 \rightarrow D^+$ beam injection was used since, in a deuterium plasma, the fusion products interact with a deuteron density which is a large fraction of the electron density. However, in terms of PLT and PDX operation, $D^0 \rightarrow H^+$ is more common (see, for instance, Ref.[2]) and, therefore, much of our data is for these conditions. For these $D^0 \rightarrow H^+$ beam injection cases the deuteron density is more uncertain so that it is difficult to make quantitative use of these data. The ratio n_d/n_e is typically of the order of 1/2 to 1/3 since considerable deuterium streams into the vessel from the beam ducts. The ^{3}He burn-up ratio was observed to be decreased by a factor ~1/2 when the fill gas was changed from deuterium to hydrogen. Since the deuterium density is still a sizeable fraction of the electron density, the $D^0 \rightarrow H^+$ data are useful for qualitative observations.

4.1. ^{3}He burn-up data

The best documented ^{3}He burn-up data are for a series of $D^0 \rightarrow D^+$ discharges on PDX at 2.2 T (Table I). The measured burn-up agrees with the predictions of classical theory over the full range of plasma currents achievable on PDX (Fig.12). As expected classically, changes in beam power between 1 and 4 MW did not influence the burn-up.

The time evolution (Fig.13) of the ^{3}He burn-up was also consistent with classical theory. For the sixteen $D^0 \rightarrow D^+$ discharges with plasma current $I_\phi \gtrsim 300$ kA the rise of the d-^{3}He reaction rate was delayed by 18 ± 10 ms with respect to the ^{3}He production rate and the fall was delayed by 11 ± 9 ms. These delays are comparable with the time required for ^{3}He ions to slow down classically through the maximum of the fusion cross-section in a 1–2 keV plasma with ~3 × 10^{13} cm^{-3} electron density.

The above discussion applies to burn-up data taken at high toroidal fields in plasmas with sawtooth MHD activity. At lower fields, a significant departure from classical burn-up was observed. In Fig.14, the dependence of the ^{3}He burn-up on toroidal field during $D^0 \rightarrow H^+$ injection is plotted. The plasma current (200 kA), central electron temperature (1.2 keV), beam power (4 MW) and electron density ($\bar{n}_e \cong 2.5 \times 10^{13}$ cm^{-3}) were nearly constant during this scan, except at 1.1 T, where the electron temperature and density fell by 25% and 40%, respectively. The soft-X-ray signals indicated m = 1, n = 1 activity

TABLE I. PDX ^{3}He BURN-UP FOR $D^0 \rightarrow D^+$ NEUTRAL BEAM INJECTION

Shot	d-^{3}He/d-d		2.5 MeV Emission rate (10^{13} n·s^{-1})	Plasma current (kA)	$\bar{n}_e$ (10^{13} cm^{-3})	$T_e(0)$ (keV)	Beam power (MW)
	Measured[a] (10^{-4})	Predicted[b] (10^{-4})					
42300	2.5	1.3	5.5	320	2.7	1.9	4.0
42301	3.0	1.2	6	320	3.3	1.9	4.0
42302	2.3	1.4	4	310	3.1	1.9	2.8
42303	1.3	1.0	1.9	300	2.2	1.6	2.9
42304	1.7	1.0	1.5	300	2.1	1.6	1.6
42309	2.7	2.2	9	430	2.8	2.5	4.1
42310	2.5	2.0	8	400	2.8	2.4	4.4
42312	3.2	2.6	6	400	2.7	2.7	4.3
42314	2.8	n.a.	10	480	3.0	n.a.	4.4
42318	0.9	0.9	4	190	2.6	2.3	4.5
42320	0.3	0.3	1.5	140	1.8	1.4	3.2
42321	0.1	0.15	0.7	130	3.1	1.3	1.7
42322	0.2	0.13	2.5	130	3.3	1.2	4.5

[a] Absolute uncertainty is ± 70%.
[b] 0.7 of the MIS code prediction; the uncertainty is a factor of two.

in the centre of the discharge, but sawteeth were generally absent. Large m = 2, n = 1 magnetic fluctuations were detected (Fig.14) by an array of Mirnov coils located outside the plasma. In contrast to theory, which predicts a weak toroidal field dependence of the burn-up, the measured ^{3}He burn-up fell

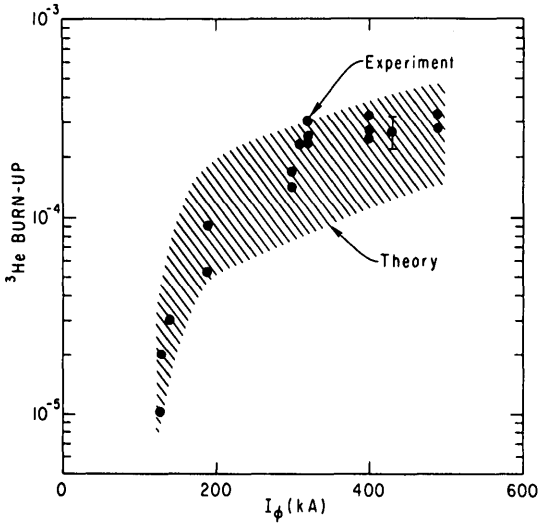

FIG.12. The ^{3}He burn-up data of Table I plotted versus plasma current. The toroidal field was 2.2 T during the scan.

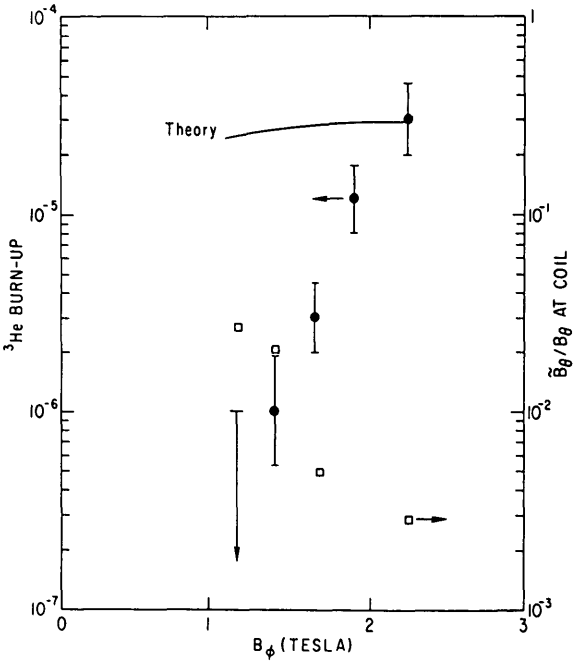

FIG.14. ^{3}He burn-up versus toroidal field during $D^0 \rightarrow H^+$ injection. With the exception of the shots at 1.1 T, the beam power, electron density, plasma current and electron temperature were approximately constant throughout the scan. The theory is the classically predicted toroidal field dependence, normalized to the 2.2 T data point. The magnetic field fluctuations had an m = 2, n = 1 mode structure. At 1.1 T, the burn-up was below the detectable level.

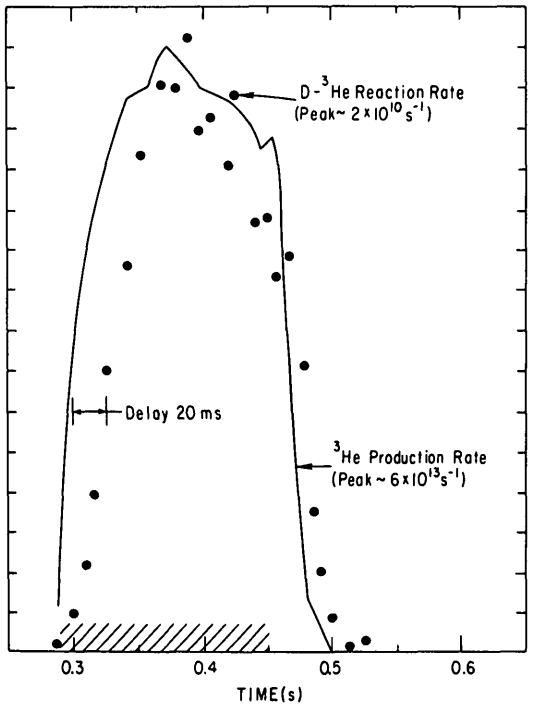

FIG.13. Time evolution of the PDX d-d and d-^{3}He emissions during $D^0 \rightarrow D^+$ beam injection (hatching).

by a factor of 100 when the toroidal field was decreased. The d-d rate fell less strongly, only by about a factor of two. (Recall that the detector efficiency was relatively insensitive to toroidal field (Fig.11).)

^{3}He burn-up measurements were also made in 2.2 T PDX discharges that did not have normal sawtooth MHD activity. In $D^0 \rightarrow H^+$ discharges with weak 'fishbone' MHD activity [12–14] (5–10% drops in neutron emission; fishbone period > 20 ms), statistically significant reductions in the d-^{3}He reaction rate at the time of the instability were absent. However, in the m = 2 discharge of Fig.15, reductions in the ^{3}He burn-up were strongly correlated with the MHD activity. The d-^{3}He reaction rate rose from the beginning of beam injection until, at 200 ms, a sudden drop occurred in the d-d reaction rate and soft-X-ray emission. The ^{3}He burn-up also dropped immediately, indicating that some 0.8 MeV ^{3}He ions were lost or rapidly decelerated. For the next ~ 70 ms, the ^{3}He burn-up was roughly a factor of two less than in equivalent sawtooth discharges. Then, after the small

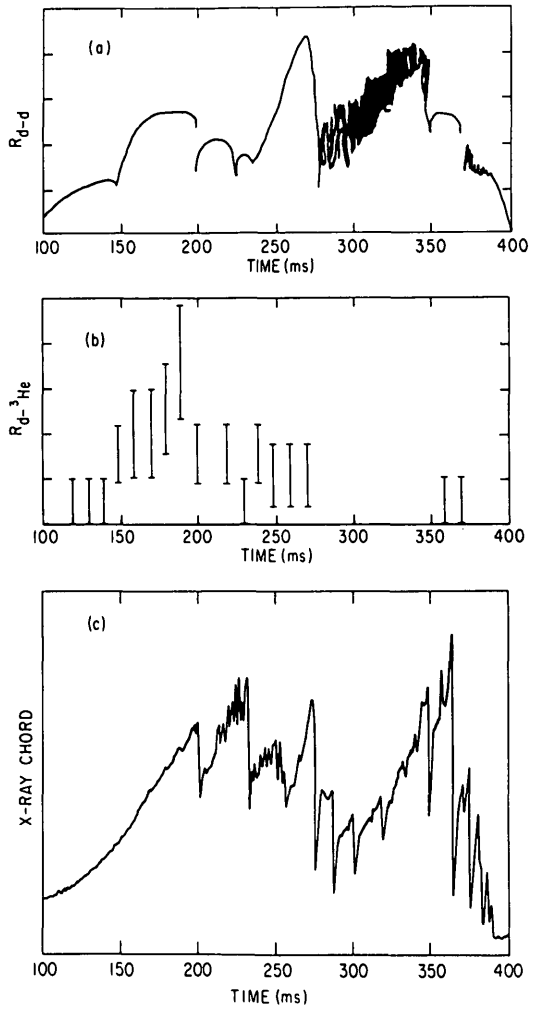

FIG.15. (a) Time evolution of the 2.4 MeV neutron emission measured with a NE422 scintillator (frequency response of 10 kHz) in a $D^0 \rightarrow H^+$ PDX discharge with m = 2 MHD activity. (b) Time evolution of the 15 MeV proton emission measured in 10 ms counting bins. (c) Time evolution of the central soft X-rays.

disruption at 270 ms, strong oscillations occurred in the neutron emission and the d-^{3}He reaction rate fell below the minimum detectable level for 80 ms, indicating a factor-of-ten reduction in the ^{3}He burn-up.

4.2. Triton burn-up data

The best documented cases of triton burn-up come from three PLT runs during $D^0 \rightarrow D^+$ neutral beam injection of about 1.5 MW of power (Table II, Figs 16, 17). In each of these runs, similar plasma conditions were maintained on each of a sequence of shots to minimize the importance of shot-to-shot irreproducibility. At 3.2 T and $I_\phi \cong 500$ kA (line 1 of Table II, Fig.16), the triton burn-up was $(6.4 \pm 0.6) \times 10^{-4}$, which is on the low end of values that are consistent with the classical predictions of the SGA code (1.2×10^{-3}). In the lower current and electron temperature discharges of line 2 of Table II, the burn-up was $(1.8 \pm 0.8) \times 10^{-4}$, a value having the same relationship to the classical prediction (2.9×10^{-4}) as the high-field 500 kA discharges. However, at 1.8 T and $I_\phi \cong 500$ kA (line 3 of Table II, Fig.17), the burn-up was $\lesssim 2 \times 10^{-5}$, a value at least ten times smaller than predicted by theory and over thirty times smaller than the burn-up at larger toroidal field. In both 500 kA runs, the discharges had large sawtooth MHD activity. The influence of the sawtooth on the d-d neutron emission was a 3% drop at 3.2 T [2] and a 15% drop at 1.8 T.

An aluminium activation sample was also exposed (line 4 of Table II) during the $D^0 \rightarrow D^+$ PDX current scan documented in Table I. Analysis of the sample showed that the d(t,n) emission was relatively large during the scan but, because the plasma parameters

TABLE II. PLT AND PDX TRITON BURN-UP FOR $D^0 \rightarrow D^+$ NEUTRAL BEAM INJECTION

Device	d-t/d-d		Current (kA)	$\bar{n}_e$ (10^{13} cm^{-3})	$T_e(0)$ (keV)	Toroidal field (T)	Comments
	Measured (10^{-4})	Predicted[a] (10^{-4})					
1. PLT	6.4 ± 0.6	12	450–500	2.5	2.2	3.2	Reproducible discharges (Fig.16)
2. PLT	1.8 ± 0.8	2.9	280–330	2	1.45	3.2	Reproducible discharges
3. PLT	<0.2	8	450–530	3.5–5	1.7	1.8	Reproducible discharges (Fig.17)
4. PDX	12[b]	10–20[b]	400–500	2–3	1–3	2.2	^{3}He burn-up current scan

[a] By the SGA code; the uncertainty is a factor of two.
[b] D-T emission divided by D-D emission of 400–500 kA discharges *only*.

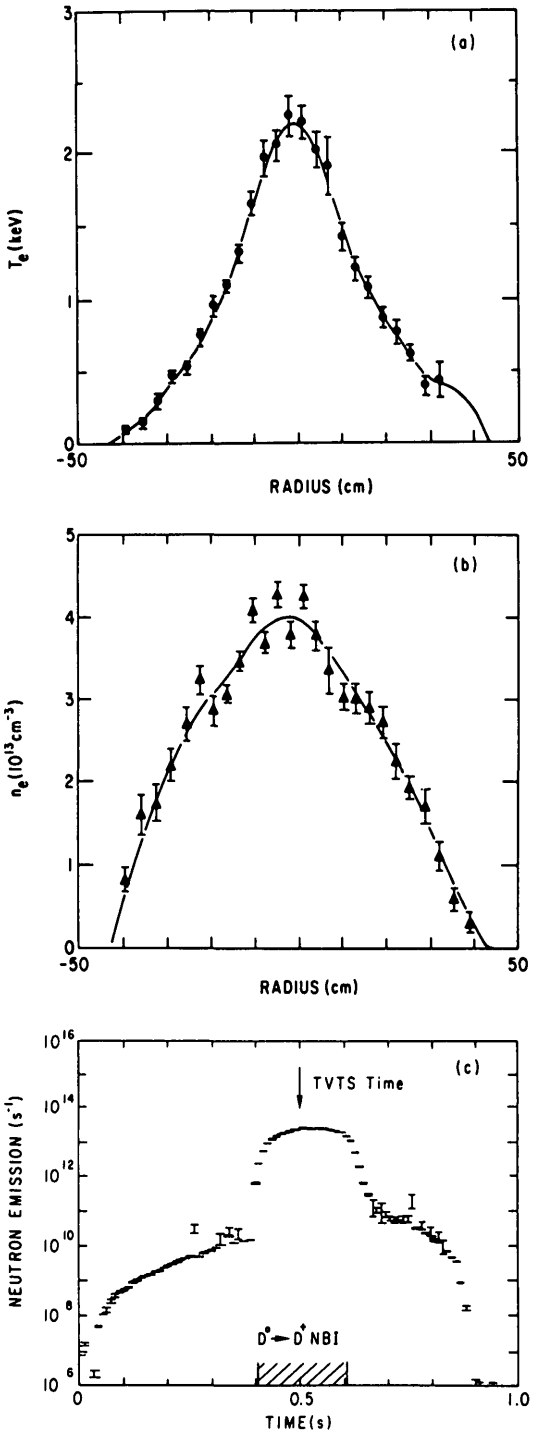

FIG.16. Thomson scattering profiles of electron temperature (a) and electron density (b), and time evolution of the 2.4 MeV neutron emission (c) for the $B_\phi = 3.2$ T, $I_\phi = 500$ kA discharges with classical triton burn-up (line 1 of Table II). The other plasma parameters were: $a = 40$ cm, $R_0 = 134$ cm, $Z_{eff} \cong 1$, and sawtooth MHD activity. Two co-beams and one counter-beam injected 1.5 MW.

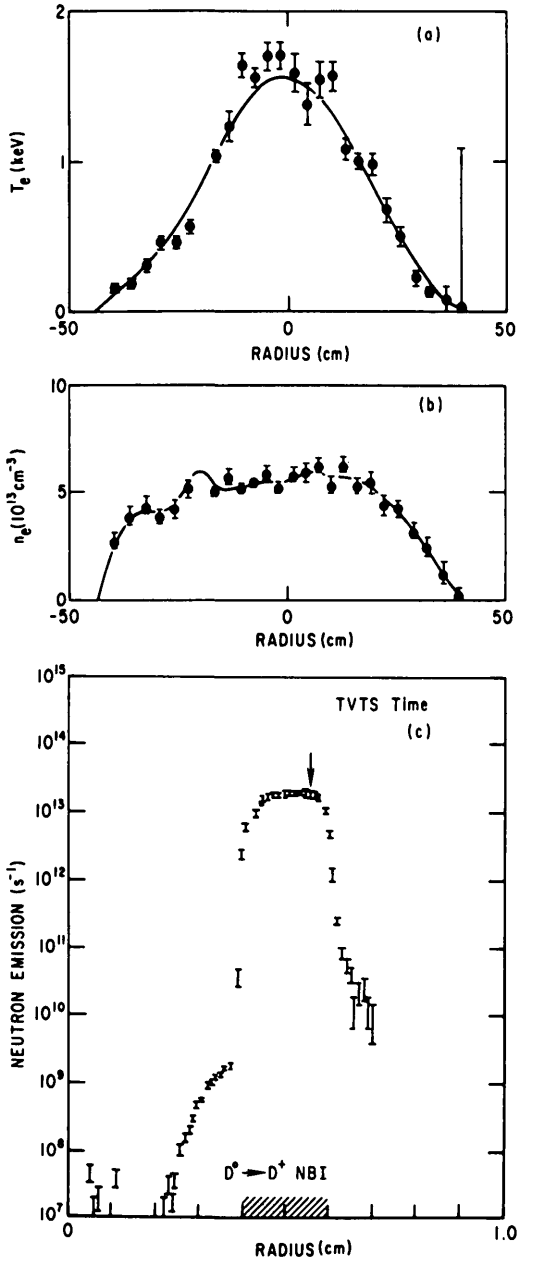

FIG.17. Thomson scattering profiles of electron temperature (a) and electron density (b), and time evolution of the 2.4 MeV neutron emission (c) for the $B_\phi = 1.8$ T, $I_\phi = 500$ kA discharges with anomalous triton burn-up (line 3 of Table II). The other plasma parameters were: $a = 40$ cm, $R_0 = 134$ cm, $Z_{eff} \cong 1$, and sawtooth MHD activity. Two co-beams and one counter-beam injected 1.8 MW.

TABLE III. PLT AND PDX TRITON BURN-UP FOR $D^0 \rightarrow H^+$ NEUTRAL BEAM INJECTION

Device	d-t/d-d (10^{-4})	Current (kA)	$\bar{n}_e$ (10^{13} cm^{-3})	Toroidal field (T)	Comments
1. PLT	1.9 ± 1.2	450	1–2	2.5	0.4% ripple
2. PLT	1.1 ± 0.6	450	1–2	2.5	2.7% ripple
3. PDX	0.8 ± 0.5	500	4–5	2.3	< 0.1% ripple
4. PDX	0.5 ± 0.4	450–500	4–5	2.3	< 0.1% ripple

were not held constant during the sample's exposure, it is not possible to determine quantitatively the triton burn-up from this measurement. Nonetheless, the measurement does indicate that the triton burn-up on PDX at 2.2 T was of the same order of magnitude as that on PLT at 3.2 T.

An attempt was made to assess the importance of ripple on the triton burn-up during $D^0 \rightarrow H^+$ injection (Table III). In addition to ~0.4% periodic field ripple, PLT has a damaged toroidal field coil that introduces slightly higher ripple at one toroidal location [15]. One experiment consisted of introducing a shunt at one toroidal location, which increased the local field well from 0.4% to 2.7% [15]. Two deuterium injection runs on one day provided a large-ripple:small-ripple comparison (lines 1 and 2 of Table III). Within experimental error, no effect on the triton burn-up was observed. Burn-up data were also collected on PDX under discharge conditions similar to those of the PLT experiments (lines 3 and 4 of Table III). PDX has less than 0.1% periodic field ripple. No significant variation in the triton burn-up was observed in any of these different ripple configurations.

A second difference between PLT and PDX is the neutral beam injection angle. The similar results obtained on PLT and PDX (lines 1 and 4 of Table II, lines 2 and 3 of Table III) indicate that the triton burn-up is not strongly dependent on beam injection angle.

The centre of the d-t emitting region of the plasma was found by simultaneously placing foils on the PLT vacuum vessel 90° above the plasma, 90° below the plasma, and on the horizontal midplane outside the plasma. The d-t flux was up-down symmetric and was about 20% higher on the horizontal midplane outside the plasma (Fig.18). The up-down symmetry of the d-t emission confirms that the d-t reactions occurred within the plasma since, if the reactions had occurred from unconfined tritons encountering deuterium in the wall, the emission would be strongly peaked toward the bottom of the plasma. The enhanced outward d-t flux indicates that the d-t emission profile was shifted outwards with respect to the vessel centre (R = 135 cm), consistent with the d-t centre being at R = 146 ± 10 cm. In a similar experiment using indium foils, the d-d emission centre was 142 ± 4 cm [9], consistent with an outward Shafranov shift of the plasma centre. The outward shift of the d-t centre indicates that the confined tritons include co-going ions since entirely counter-going ions would feature an inward shift.

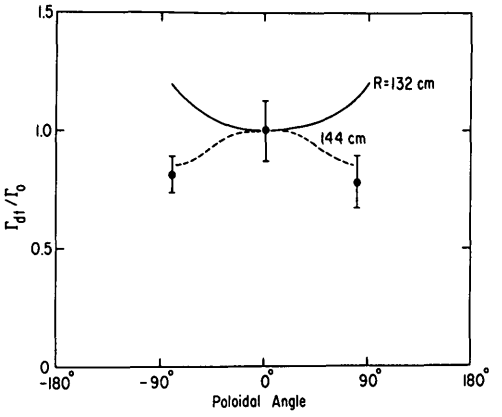

FIG.18. 14 MeV neutron flux through the PLT vacuum vessel as a function of poloidal angle; 0° is on the horizontal midplane outside the plasma, 90° is vertically above the plasma. The curves indicate the expected poloidal symmetry for toroids with major radii of 132 and 144 cm, respectively [9].

Attempts to measure the triton burn-up with an NE213 scintillator also were made during $D^0 \rightarrow H^+$ neutral beam injection. The recoil proton spectra from these measurements did not contain a 14 MeV edge,

indicating a triton burn-up of less than 3×10^{-4}, which agrees with the burn-up measured concurrently using activation techniques (Table III).

5. DISCUSSION

5.1. Fusion product burn-up at high toroidal fields

The agreement between the magnitude, current dependence and time evolution of the experimentally observed burn-up and the classical predictions indicate that in high toroidal field discharges the ^{3}He ion burn-up was classical (within about a factor of two). This implies that in these discharges the 0.8 MeV ^{3}He confinement time was $\gtrsim 15$ ms and that the rate of energy loss was close to the classical energy loss rate. In other high toroidal field discharges, characterized by large m = 2 MHD activity and rapid drops in the neutron emission, significant drops in the ^{3}He burn-up were observed, indicating that ^{3}He ions were lost or rapidly decelerated during these events.

The measured triton burn-up (6.4×10^{-4} at 500 kA, 1.8×10^{-4} at 300 kA) at 3.2 T is within a factor of two of the predictions of the SGA code. This implies that in these discharges the 1.0 MeV triton confinement time was $\gtrsim$ 100 ms and that the rate of energy loss was close to the classical loss rate. The reduced burn-up in the 300 kA case is explained classically as being due to a factor-of-three reduction in triton confinement at lower plasma current (Fig.3). Theoretically, the burn-up probability for confined tritons was not significantly reduced in the lower-current case because the effect of the lower electron temperatures was partially cancelled by the effect of a longer (300 ms) beam pulse that permitted a larger fraction of confined tritons to slow down through the peak of the fusion cross-section before the temperature fell to its Ohmic level.

Reference [1] reports a PLT triton burn-up of 5×10^{-3} at I_ϕ = 500 kA and of 3×10^{-3} at I_ϕ = 250 kA, accurate to within a factor of four. The data of Ref.[1] were obtained with a large NE213 scintillator and a ^{7}Li glass scintillator. The ^{7}Li glass scintillator results may have been contaminated by epithermal neutrons [16] and should be discounted. The NE213 measurements of Ref.[1] remain valid, however.

Although most of the factor-of-ten difference between the results reported here and those of Ref.[1] is probably due to improvements in diagnostic accuracy, it is also possible that changes in plasma conditions account for some of the difference. The early PLT results were obtained during 650 kW of $H^0 \rightarrow D^+$ injection, while the results reported here were obtained with 1.5 MW of $D^0 \rightarrow D^+$ injection. Although the ratio n_d/n_e is smaller for $H^0 \rightarrow D^+$, causing a reduction in triton burn-up, the triton birth distribution is expected to be more highly peaked for $H^0 \rightarrow D^+$, which should enhance the triton burn-up (Fig.5). It is also possible that injection of a heavier species at higher power affected the triton confinement by changing the plasma rotation velocity. A second change in PLT conditions is that the previous results were obtained before the toroidal field coil damage which left a permanent well at one toroidal location. The negative results of the large-ripple:small-ripple comparison (Table III), together with the fact that the theoretical predictions assume that all trapped tritons are lost in PLT even in the absence of ripple (Fig.19), suggest that this change, however, is not responsible for a major change in triton burn-up. We conclude that the greater accuracy of activation techniques probably accounts for most of the difference between the results reported here and those reported in Ref.[1].

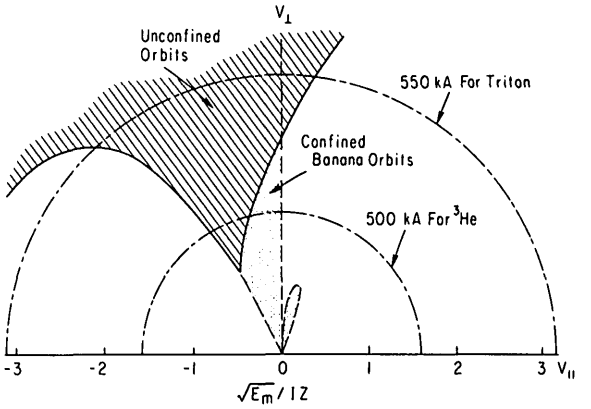

FIG.19. Loss [5] and trapping [3] boundaries in velocity space for guiding centres born at $R_i/R_0 = 1.07$, $z_i = 0$ in PLT ($a/R_0 = 0.30$). A current profile $[j \propto 1-(r^2/a)]^4$ is assumed, and guiding centres that strike the limiter are considered lost. The units of $\sqrt{Em}/IZ$ are $[MeV]^{1/2} \cdot [MA]^{-1} \cdot [amu]^{1/2}$.

5.2. Toroidal field dependence

Classically, one expects the burn-up to decrease slightly as the toroidal field is decreased. To leading order in the small parameter (B_θ/B_ϕ), particle drift orbits are independent of toroidal field in a tokamak, so the only effect of a reduction in toroidal field on a

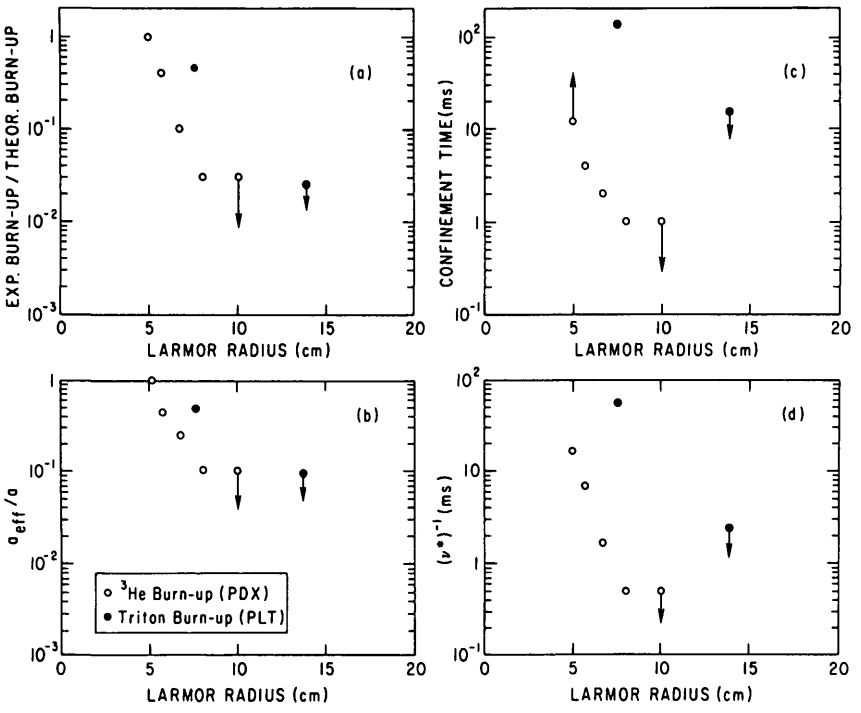

FIG.20. Application of the anomalous burn-up models (Sect.2.2) to the experimental data, plotted as a function of Larmor radius. (a) Measured burn-up divided by the predicted burn-up, (b) prompt loss model, (c) diffusive loss model, (d) anomalous slowing-down model. Arrows pointing down (up) represent a value less than (greater than) or equal to the plotted point.

particle's orbit is an increase in its gyroradius. If the toroidal field is halved, one expects the burn-up to drop by about a factor of two, owing to finite gyroradius effects (Fig.4, Sect. 2.1). Experimentally, however, halving the toroidal field reduced the fusion product burn-up by more than an order of magnitude. Clearly, physical mechanisms not included in the classical theory were operative during the experiments.

One effect of a reduction in toroidal field is to increase the radius of the q = 1 surface. This suggests the possibility that the broader sawtooth region for low-q discharges allows direct fusion product losses at internal disruptions. In the 1.8 T PLT discharges (line 3 of Table II) the radial extent of the sawtooth event was within a triton gyroradius of the limiter. Internal disruptions were absent during the scan of the toroidal field dependence of the ^{3}He burn-up.

A second possibility is that the change in toroidal field modified the state of plasma turbulence and thereby promoted loss of the fusion products.

Another effect of a reduction in toroidal field is to increase the ion gyroradius. Hinton [17] has predicted that intrinsic orbit stochasticity can occur over most of phase space owing to resonances between the gyromotion and free-streaming motion of a particle for large gyroradii particles in a machine with significant ripple. These stochastic orbits, if they exist, would allow particles to escape from the torus on a short time-scale. Application of Hinton's stochasticity criterion to the 1 MeV triton in PLT indicates that at 1.8 T the triton is near the stochasticity threshold, while at 3.2 T in PLT the triton orbits are integrable. Although this effect can account for the triton burn-up observations, it cannot account for the reduction in ^{3}He burn-up, since the smaller PDX ripple and the smaller ^{3}He gyroradius place the ^{3}He ion well below Hinton's threshold for stochasticity. We note, however, that other magnetic field perturbations, such as the relatively large helical field detected by the Mirnov coils in the ^{3}He burn-up toroidal field scan, may affect large gyroradii particles in a manner analogous to the rippled field structure considered by Hinton.

If one assumes that the same physical mechanism reduced both the triton and the ^{3}He burn-up, then one might expect that the mechanism is related to the

fusion product Larmor radius. In Fig.20, the burn-up data are plotted in terms of each of the equivalent anomalous burn-up parameters (Sect. 2.2). These parameters are: (a) the burn-up reduction, (b) the effective loss radius which models a prompt-loss mechanism, (c) the confinement time which represents a diffusive loss mechanism, and (d) the effective slowing-down time. The assumption that both ions can be explained by the same process effectively rules out anomalous diffusion or slowing down since, classically, tritons take about ten times longer to burn up than ^{3}He ions. The data (Fig.19(a, b)) suggest that a mechanism (such as intrinsic orbit stochasticity) which causes the prompt loss of fusion products in some parts of phase space while scarcely affecting confined regions is responsible for the degraded fusion product burn-up.

6. CONCLUSION

Within experimental and theoretical error, the burn-up of the fusion-produced 0.8 MeV ^{3}He ion and 1 MeV triton was classical in discharges with large toroidal field and sawtooth MHD activity. In discharges with different MHD behaviour, large drops in the ^{3}He burn-up were observed, probably due to losses of these fast ions.

Both the ^{3}He and the triton burn-up dropped by an order of magnitude when the toroidal field was reduced. The data suggest that an anomalous prompt loss mechanism may be responsible for the reduced burn-up.

No definite conclusions concerning fusion product confinement in a tokamak reactor can be drawn from a study of fusion product burn-up in PLT and PDX, since the ratio of MeV ion orbit size to system size, the MeV ion concentration and the bulk plasma properties all differ substantially in PLT and PDX from those anticipated in a tokamak reactor. Similar experimental work on larger devices and an understanding of the mechanisms responsible for reduced burn-up at reduced toroidal field are required before predictions of alpha confinement in a reactor can be made.

ACKNOWLEDGEMENTS

The authors thank J. Hosea and the PLT group, and K. Bol and the PDX group for their help in performing this study. They thank especially N. Bretz and C. Daughney for the PLT Thomson scattering data, D. Johnson and B. Grek for the PDX Thomson scattering profiles, and D. Buchenauer and K. McGuire for the PDX MHD data. The authors have benefitted from discussions with R. Goldston. Computational assistance by J. Hovey and technical assistance by G. Estepp are gratefully acknowledged.

This work was supported by the United States Department of Energy Contract No. DE-AC02-76-CHO3073.

REFERENCES

[1] COLESTOCK, P.L., STRACHAN, J.D., ULRICKSON, M., CHRIEN, R., Phys. Rev. Lett. **43** (1979) 768.
[2] STRACHAN, J.D., COLESTOCK, P.L., DAVIS, S.L., EAMES, D., EFTHIMION, P.C., et al., Nucl. Fusion **21** (1981) 67.
[3] GOLDSTON, R., Ph.D. Thesis, Ch.2, Princeton University, 1977.
[4] SPITZER, L., Physics of Fully Ionized Gases, Interscience, New York (1962).
[5] HIVELY, L.M., MILEY, G.M., Nucl. Fusion **17** (1977) 1031.
[6] PETRIE, T.W., MILEY, G.M., IEEE Trans. Plasma Sci. **PS-8** (1980) 101.
[7] HIVELY, L.M., MILEY, G.M., Nucl. Fusion **20** (1980) 969.
[8] ULRICKSON, M., Triton Confinement and 14 MeV Neutron Production in PLT, Princeton Plasma Physics Lab. Rep. TM-291 (1976).
[9] ZANKL, G., STRACHAN, J.D., LEWIS, R., PETTUS, W., SCHMOTZER, J., Nucl. Instrum. Meth. **185** (1981) 321.
[10] CHRIEN, R.E., COLESTOCK, P.L., EUBANK, H.P., HOSEA, J.C., HWANG, D.Q., STRACHAN, J.D., THOMPSON, H.R., Jr., Phys. Rev. Lett. **46** (1981) 535.
[11] CHRIEN, R.E., EUBANK, H.P., MEADE, D.M., STRACHAN, J.D., Nucl. Fusion **21** (1981) 1661.
[12] BELL, M., ARUNASALAM, V., BITTER, M., BLANCHARD, W., BOL, K., et al., in Controlled Fusion and Plasma Physics (Proc. 10th Europ. Conf. Moscow, 1981) Vol.2, Sovintsentr, Moscow (1981) 16.
[13] JOHNSON, D., BELL, M., BITTER, M., BOL, K., BRAU, K., et al., in Plasma Physics and Controlled Nuclear Fusion Research 1982 (Proc. 9th Int. Conf. Baltimore, 1982) Vol.1, IAEA, Vienna (1983) 9.
[14] McGUIRE, K., GOLDSTON, R., BELL, M., BITTER, M., BOL, K., et al., Phys. Rev. Lett. **50** (1983) 891.
[15] STODIEK, W., GOLDSTON, R., SAUTHOFF, N., ARUNASALAM, V., BARNES, C., et al., in Plasma Physics and Controlled Nuclear Fusion Research 1980 (Proc. 8th Int. Conf. Brussels, 1980) Vol.1, IAEA, Vienna (1981) 9.
[16] CHRIEN, R.E., Ph.D. Thesis, Princeton University, 1982, 32.
[17] HINTON, F.L., Plasma Phys. **23** (1981) 1143.

(Manuscript received 16 August 1982
Final manuscript received 5 May 1983)